Localized bulging in an inflated cylindrical tube of arbitrary thickness – the effect of bending stiffness

Y.B. Fu, J.L. Liu, G.S. Francisco

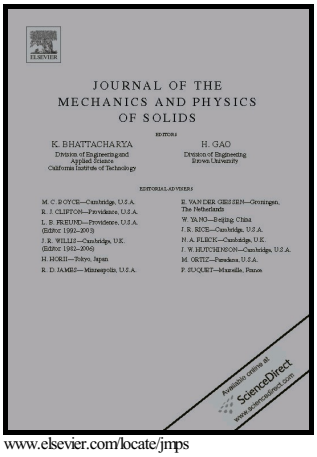

www.elsevier.com/locate/jmps

PII: S0022-5096(15)30261-1
DOI: http://dx.doi.org/10.1016/j.jmps.2016.02.027
Reference: MPS2820

To appear in: *Journal of the Mechanics and Physics of Solids*

Received date: 17 November 2015
Revised date: 27 January 2016
Accepted date: 1 February 2016

Cite this article as: Y.B. Fu, J.L. Liu and G.S. Francisco, Localized bulging in an inflated cylindrical tube of arbitrary thickness – the effect of bending stiffness *Journal of the Mechanics and Physics of Solids* http://dx.doi.org/10.1016/j.jmps.2016.02.027

Localized bulging in an inflated cylindrical tube of arbitrary thickness – the effect of bending stiffness

Y.B. Fu[a,b,*], J.L. Liu[a], G.S. Francisco[b]

[a] *Department of Mechanics, Tianjin University, Tianjin 300072, China*
[b] *Department of Mathematics, Keele University, Staffordshire ST5 5BG, UK*

Abstract

We study localized bulging of a cylindrical hyperelastic tube of *arbitrary thickness* when it is subjected to the combined action of inflation and axial extension. It is shown that with the internal pressure P and resultant axial force F viewed as functions of the azimuthal stretch on the inner surface and the axial stretch, the bifurcation condition for the initiation of a localized bulge is that the Jacobian of the vector function (P, F) should vanish. This is established using the dynamical systems theory by first computing the eigenvalues of a certain eigenvalue problem governing incremental deformations, and then deriving the bifurcation condition explicitly. The bifurcation condition is valid for all loading conditions, and in the special case of fixed resultant axial force it gives the expected result that the initiation pressure for localized bulging is precisely the maximum pressure in uniform inflation. It is shown that even if localized bulging cannot take place when the axial force is fixed, it is still possible if the axial stretch is fixed instead. The explicit bifurcation condition also provides a means to quantify precisely the effect of bending stiffness on the initiation pressure. It is shown that the (approximate) membrane theory gives good predictions for the initiation pressure, with a relative error less than 5%, for thickness/radius ratios up to 0.67. A two-term asymptotic bifurcation condition for localized bulging that incorporates the effect of bending stiffness is proposed, and is shown to be capable of giving extremely accurate predictions for the initiation pressure for thickness/radius ratios up to as large as 1.2.

Keywords: Localized bulging, rubber tubes, aneurysm, bifurcation, nonlinear elasticity.

1. Introduction

Localized bulging in an inflated cylindrical hyperelastic tube is characterized by three distinct phases: initiation, growth and propagation, which are also shared by a large variety of other localization problems in continuum mechanics. It is therefore a fundamental protypical problem whose understanding can help shed light on other more complicated localization problems. The problem itself is relevant to a variety of applications, as witnessed by a series

*Corresponding author at: Department of Mathematics, Keele University, Staffordshire ST5 5BG, UK
Email address: y.fu@keele.ac.uk (Y.B. Fu)

of recent studies on the continuum-mechanical modelling of aneurysm initiation in human arteries (Fu et al., 2012; Alhayani et al., 2013, 2014; Rodrguez-Martnez et al., 2015), and on localized bulging under the additional effects of swelling (Demirkoparan & Merodio, 2015), viscoelasticity/chemorheology (Wineman, 2015a,b), and electric actuation (Lu et al., 2015).

Localized bulging in an inflated isotropic rubber tube was first documented by Mallock (1891), and later studied experimentally and numerically by Kyriakides & Chang (1990, 1991), Pamplona et al. (2006), Goncalves et al. (2008), and Shi & Moita (1996). The propagation stage was recognized by Yin (1977) and Chater & Hutchinson (1984) as a two-phase deformation governed by Maxwell's equal area rule, but the character of the initiation stage, and its connection with the so-called limit-point instability (Alexander, 1971; Kanner & Horgan, 2007), was not fully understood until more recently. In the early stability and buckling analysis of a hyperelastic cylindrical tube that is subjected to the combined action of internal inflation and axial stretching/compression, attention was mainly focused on periodic perturbations/patterns (Shield, 1972; Haughton & Ogden, 1979a,b; Chen, 1997). The special case when the axial mode number is zero was thought to correspond to a bifurcation into another uniformly inflated configuration, and thus to have no relevance to localized bulging. However, it was recognized by Fu et al. (2008) and Pearce & Fu (2010) that it is precisely this zero mode number case that corresponds to localized bulging when nonlinear effects are brought into play. It was further shown in Fu & Il'ichev (2015) that in the case of fixed resultant axial force (hereafter simply referred to as *axial force*), the initiation pressure for localized bulging corresponds to the maximum pressure in uniform inflation, but this correspondence may no longer hold when other loading conditions are applied at the ends. In particular, when the axial stretch is fixed during inflation, localized bulging may occur even if the pressure in uniform inflation does not have a maximum. Whether localized bulging can take place or not is also dependent on the material models used, and this issue was examined by Pearce (2012). Stability of the localized bulging configuration in the growth stage was studied by Fu & Xie (2010) and Il'ichev & Fu (2012), whereas imperfection sensitivity of localized bulging have recently been examined by Fu & Xie (2012).

In most of the above-mentioned studies, the tube is modeled as a membrane without any bending stiffness. In the present paper, we address the following questions: (1) would localized bulging occur in a pressurized cylindrical tube of *any thickness*? (2) how does bending stiffness affect the initiation pressure? and (3) what is the range of validity of the traditional membrane theory? Our research is mainly motivated by possible applications to the mathematical modeling of aneurysm initiation; in that context the human arteries exhibit noticeable bending stiffness in contrast with party balloons (Fung et al., 1979; Gasser et al., 2006).

When the tube is of arbitrary thickness, any nonlinear analysis would become extremely difficult, if not intractable, but fortunately, the dynamical systems theory's view provides us with a means to determine the bifurcation point analytically. To sketch the idea, suppose

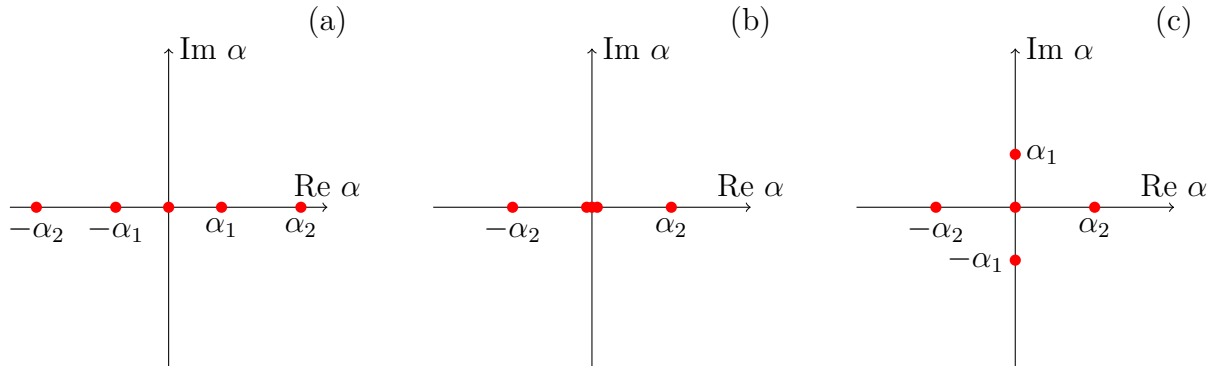

Figure 1: Movement of the five eigenvalues that are initially real as the azimuthal stretch increases. The three plots (a), (b) and (c) correspond to when the azimuthal stretch is smaller than, equal to, or greater than its critical value, respectively. Localized bulging occurs when α_1 vanishes, making zero a triple eigenvalue.

that we consider an axially symmetric perturbation superimposed on a uniformly inflated cylindrical tube. The incremental boundary value problem is readily available from the classical paper by Haughton & Ogden (1979b). Suppose now further that the perturbation depends on the axial coordinate z through $\mathrm{e}^{\alpha z}$. Then the incremental boundary value problem reduces to the form given by (3.2) and (3.3). This is an eigenvalue problem and we may look for eigenvalues of α such that non-trivial solutions can be found. We observe that part of Haughton & Ogden (1979b)'s numerical computation was concerned with solutions of this eigenvalue problem when α is replaced by $-\mathrm{i}\alpha$ where $\mathrm{i} = \sqrt{-1}$. It can be shown that the distribution of eigenvalues is symmetric with respect to both axes in the complex α-plane. Suppose that we characterize the uniform inflation using the azimuthal stretch λ_a on the inner surface. When λ_a is increased only slightly above 1, it can be shown that there are five real eigenvalues of α of the form $0, \pm\alpha_1, \pm\alpha_2$ such that $0 < \alpha_1 < \alpha_2$; see Fig.1(a). As λ_a increases, the two real eigenvalues $\pm\alpha_1$ will move towards the origin. When they eventually coalesce at the origin, zero becomes a triple eigenvalue which signals the initiation of a bifurcation into a localized solitary-wave type solution (Kirchgässner, 1982; Mielke, 1991; Haragus & Iooss, 2011). When λ_a is increased further, the two eigenvalues $\pm\alpha_1$ would move onto the imaginary axis. The exponential $\mathrm{e}^{\alpha z}$ then becomes sinusoidal, and this is the situation addressed by Haughton & Ogden (1979b). It is clear from this deduction that localized bulging must necessarily occur before any bifurcation into periodic patterns. This fact is consistent with all experimental observations (Kyriakides & Chang, 1990, 1991; Pamplona et al., 2006; Goncalves et al., 2008).

Thus, determination of the initiation pressure is reduced to finding the condition under which zero becomes a triple eigenvalue of the eigenvalue problem (3.2) and (3.3). Since it is known that when the membrane theory is used and in the case of fixed axial force, this coalescence of eigenvalues at the origin corresponds precisely to when the pressure in uniform inflation reaches its maximum, it is natural to ask whether this correspondence can

be extended to the case when the exact theory of nonlinear elasticity is used. This is found to be indeed the case.

We organize the rest of the paper as follows. After formulating the incremental problem in the next section, we solve the above-mentioned eigenvalue problem numerically for general real α in Section 3, and analytically for small α in Section 4. In both sections, it is verified that in the case of fixed axial force zero becomes a triple eigenvalue when the pressure attains its maximum in uniform inflation. It is further deduced that the bifurcation condition corresponds to the fact that the Jacobian of the pressure and axial force becomes zero when they are viewed as functions of the azimuthal stretch on the inner surface and the axial stretch. In Section 5, the initiation pressure is computed using both the membrane theory and the exact 3D theory, and the effect of bending stiffness is then quantified. We also plot the bifurcation condition as a curve in the pressure/axial stretch plane so that the effects of axial stretch are graphically displayed. This enables us to make a direct comparison with the experimental results reported in Goncalves et al. (2008). In Section 6 we propose a two-term asymptotic bifurcation condition for computing the initiation pressure; the first term corresponds to the membrane theory whereas the second term incorporates the effect of bending stiffness. The paper is then concluded with a summary and additional discussions.

2. Problem formulation

Our point of departure is the paper by Haughton & Ogden (1979b). We first recall some results from this paper which are necessary for our subsequent analysis.

Consider a hyperelastic cylindrical tube that initially has inner radius A and outer radius B. When it is uniformly stretched in the axial direction and inflated by an internal pressure P, the inner and outer radii become a and b, respectively. In terms of cylindrical polar coordinates, the deformation is given by

$$r^2 = \lambda_z^{-1}(R^2 - A^2) + a^2, \quad \theta = \Theta, \quad z = \lambda_z Z, \tag{2.1}$$

where (R, Θ, Z) and (r, θ, z) are the coordinates in the undeformed and deformed configurations, respectively, and λ_z is the stretch in the axial direction which is assumed to be a constant throughout this paper.

With incompressibility taken into account, the three principal stretches are given by

$$\lambda_1 \equiv \lambda = \frac{r}{R}, \quad \lambda_2 = \lambda_z, \quad \lambda_3 = 1/(\lambda_1\lambda_2),$$

where the first equation defines λ as a function of r (with R eliminated using $(2.1)_1$). Following Haughton & Ogden (1979b), we have identified the indices $1, 2, 3$ with the θ-, z-, and r-directions, respectively.

We assume that the constitutive behavior of the tube is described by a strain-energy function $W(\lambda_1, \lambda_2, \lambda_3)$. In terms of the reduced strain-energy function w defined by

$$w(\lambda, \lambda_z) = W(\lambda, \lambda_z, \lambda^{-1}\lambda_z^{-1}), \tag{2.2}$$

the internal pressure is given by

$$P = \int_{\lambda_b}^{\lambda_a} \frac{w_1}{\lambda^2\lambda_z - 1} d\lambda, \tag{2.3}$$

where $w_1 = \partial w/\partial\lambda$, and the two limits λ_a and λ_b are defined by

$$\lambda_a = \frac{a}{A}, \quad \lambda_b = \frac{b}{B},$$

and are related to each other by

$$\lambda_a^2\lambda_z - 1 = \frac{B^2}{A^2}(\lambda_b^2\lambda_z - 1). \tag{2.4}$$

The three principal stresses are

$$\sigma_{ii} = \sigma_i - \bar{p}, \quad \sigma_i = \lambda_i \frac{\partial W}{\partial \lambda_i}, \text{ no summation on } i, \tag{2.5}$$

where $\bar{p}$ is the pressure associated with the constraint of incompressibility.

The resultant axial force at any cross section is independent of Z and is given by

$$F(\lambda_a, \lambda_z) \equiv 2\pi \int_a^b \sigma_{22} r dr - \pi a^2 P = \pi A^2(\lambda_a^2\lambda_z - 1) \int_{\lambda_b}^{\lambda_a} \frac{2\lambda_z w_2 - \lambda w_1}{(\lambda^2\lambda_z - 1)^2} \lambda d\lambda, \tag{2.6}$$

where $w_2 = \partial w/\partial\lambda_z$ and we have shown F explicitly as a function of λ_a and λ_z (the λ_b in the equation is eliminated using (2.4)).

We shall assume that the tube is long enough so that the end effects can be neglected and we focus on the main section of the tube away from either of the two ends. Thus, for our purpose the tube is effectively infinitely long. We shall also assume that during inflation either the axial force F or axial stretch λ_z is fixed. The former corresponds to the situation when one end is fixed but the other end is closed and free to move, and may or may not be subjected to the extra pulling of a dead weight. Such a setup was used in the experiments of Kyriakides & Chang (1991). This is also how one would usually inflate a tubular party balloon. In this case the equation $F = C$, where C is a constant, can be solved to express λ_z in terms of λ. The latter case of a fixed axial stretch corresponds to the situation when the tube is first subjected to an axial extension and then both ends are fixed. Such a setup was used in the experiments of Goncalves et al. (2008), and is also how arteries are in situ.

The volume ratio v, that is the internal volume in the deformed configuration divided by the internal volume in the undeformed configuration, is given by $v = \lambda_z\lambda_a^2$. This quantity is a function of λ_a only since λ_z is either fixed or eliminated with the use of $F = C$. Thus, once the strain-energy function is specified, we may easily plot the dependence of P on v. In particular, when $F = C$, a pressure maximum in such a plot would correspond to

$$\left.\frac{dP}{d\lambda_a}\right|_{\text{fixed}F} = \frac{\partial P}{\partial \lambda_a} + \frac{\partial P}{\partial \lambda_z}\frac{d\lambda_z}{d\lambda_a} = 0. \tag{2.7}$$

The ordinary derivative in the above expression can be eliminated by solving

$$\frac{\partial F}{\partial \lambda_a} + \frac{\partial F}{\partial \lambda_z}\frac{d\lambda_z}{d\lambda_a} = 0. \tag{2.8}$$

It thus follows that at a pressure maximum we have

$$\frac{\partial P}{\partial \lambda_a} - \frac{\partial P}{\partial \lambda_z}\frac{\partial F}{\partial \lambda_a}\left(\frac{\partial F}{\partial \lambda_z}\right)^{-1} = 0. \tag{2.9}$$

This equation can then be solved in conjunction with $F(\lambda_a, \lambda_z) = C$ to find the values of λ_a and λ_z at which a pressure maximum in uniform inflation is attained. When these two equations do not have a solution, the pressure will be a monotonic function of the internal volume. One practical way to determine whether a pressure maximum exists or not is to draw the contour plots of the two equations together in the (λ_a, λ_z)-plane. If, for instance, there are two intersections, the pressure has both a maximum and a minimum. The existence of a pressure maximum in uniform inflation is known as a *limit-point* instability (Alexander, 1971; Kanner & Horgan, 2007). For the majority of material models, equation (2.9) together with $F = 0$ has two roots, corresponding to the fact that the pressure versus volume curve has an N shape with a maximum and a minimum. Notable exceptions are the neo-Hookean and Mooney-Rivlin material models.

In a similar manner, we may consider the variation of F with respect to λ_z when P is fixed and the latter fact is used to express λ_a in terms of λ_z. In this case the F will reach a maximum when

$$\frac{\partial F}{\partial \lambda_z} - \frac{\partial F}{\partial \lambda_a}\frac{\partial P}{\partial \lambda_z}\left(\frac{\partial P}{\partial \lambda_a}\right)^{-1} = 0. \tag{2.10}$$

We remark that in writing down (2.9) and (2.10) we have implicitly assumed that $\partial F/\partial \lambda_z$ and $\partial P/\partial \lambda_a$ are non-zero. It can be shown that in the undeformed state when $\lambda_a = \lambda_z = 1$ this is indeed the case since we then have

$$\frac{\partial F}{\partial \lambda_z} = 3\mu\pi(1 - A^2), \qquad \frac{\partial P}{\partial \lambda_a} = 2\mu\pi(1 - A^2),$$

where μ is the ground state shear modulus. It seems that none of the well-known constitutive assumptions guarantee that this is the case for all deformations, but it is known that under the membrane assumption $\partial P/\partial \lambda_a$ is at least positive before the condition for localized bulging is satisfied (Fu & Il'ichev, 2015). In the present 3D setting, for each material model that we use the above assumption is checked numerically by inspecting the contour plots of $\partial F/\partial \lambda_z = 0$ and $\partial P/\partial \lambda_a = 0$ in the (λ_a, λ_z)-plane. We have verified that this assumption is always satisfied at least before the bifurcation condition for localized bulging is satisfied.

It can be seen that both (2.9) and (2.10) imply the following equation:

$$J(P, F) \equiv \frac{\partial P}{\partial \lambda_a}\frac{\partial F}{\partial \lambda_z} - \frac{\partial P}{\partial \lambda_z}\frac{\partial F}{\partial \lambda_a} = 0, \tag{2.11}$$

which states that the Jacobian of the vector function (P, F) vanishes. It will be shown later that this is in fact the bifurcation condition for the initiation of a localized bulge whether it is the axial force or the axial stretch that is fixed.

To study the bifurcation of the primary deformation determined above, we consider an axially symmetric perturbation of the form

$$\dot{\boldsymbol{r}} = u(r,z)\boldsymbol{e}_r + v(r,z)\boldsymbol{e}_z,$$

where $\dot{\boldsymbol{r}}$ denotes the perturbation of the position vector $\boldsymbol{r}$, and $\boldsymbol{e}_r$ and $\boldsymbol{e}_\theta$ are the base vectors in the r- and θ-directions, respectively. The linearized incremental equilibrium equations that are not satisfied automatically are

$$\chi_{3j,j} + \frac{1}{r}(\chi_{33} - \chi_{11}) = 0, \quad \chi_{2j,j} + \frac{1}{r}\chi_{23} = 0, \tag{2.12}$$

where the incremental stress tensor (χ_{ij}) is given by

$$\chi_{ij} = \mathcal{B}_{jilk}\eta_{kl} + \bar{p}\eta_{ji} - p^*\delta_{ji}. \tag{2.13}$$

In the last equation, $\bar{p}$ has already been defined in (2.5), p^* is the incremental pressure field, the $\boldsymbol{\eta}$, with components η_{kl}, is the gradient of incremental displacement and is given by

$$\boldsymbol{\eta} = \begin{bmatrix} \frac{u}{r} & 0 & 0 \\ 0 & v_z & v_r \\ 0 & u_z & u_r \end{bmatrix}, \quad v_z \equiv \frac{\partial v}{\partial z}, \quad v_r \equiv \frac{\partial v}{\partial r} \text{ etc}, \tag{2.14}$$

and the $\mathcal{B}_{jilk}$'s are the instantaneous elastic moduli given by

$$\mathcal{B}_{iijj} = \mathcal{B}_{jjii} = \lambda_i\lambda_j W_{ij}, \text{ no summation on } i \text{ or } j,$$

$$\mathcal{B}_{ijij} = \frac{\lambda_i W_i - \lambda_j W_j}{\lambda_i^2 - \lambda_j^2}\lambda_i^2, \quad \lambda_i \neq \lambda_j, \text{ no summation on } i \text{ or } j,$$

$$\mathcal{B}_{ijji} = \mathcal{B}_{ijij} - \lambda_i W_i, \quad i \neq j, \text{ no summation on } i \text{ or } j,$$

where $W_i = \partial W/\partial\lambda_i$, $W_{ij} = \partial^2 W/\partial\lambda_i\partial\lambda_j$ etc.

The incompressibility condition takes the form

$$\operatorname{tr}\boldsymbol{\eta} = u_r + v_z + \frac{u}{r} = 0. \tag{2.15}$$

The incremental boundary conditions are

$$(\boldsymbol{\chi}\boldsymbol{n} - P\boldsymbol{\eta}^T\boldsymbol{n})\big|_{r=a} = 0, \quad \boldsymbol{\chi}\boldsymbol{n}|_{r=b} = 0, \tag{2.16}$$

where $\boldsymbol{n}$ denotes the normal to the surface where each of the boundary conditions is imposed. These conditions reflect the fact that the internal boundary $r = a$ is subjected to a *hydrostatic* pressure P whereas the outer boundary $r = b$ is traction-free.

Written out explicitly, the equilibrium equations (2.12) take the form

$$p_r^* = (r\mathcal{B}'_{1133} - \mathcal{B}_{1111})\frac{u}{r^2} + (r\mathcal{B}'_{3333} + r\bar{p}' + \mathcal{B}_{3333})\frac{u_r}{r} + \mathcal{B}_{3333}u_{rr} + \mathcal{B}_{2323}u_{zz}$$

$$+(r\mathcal{B}'_{2233} + \mathcal{B}_{2233} - \mathcal{B}_{1122})\frac{v_z}{r} + (\mathcal{B}_{2233} + \mathcal{B}_{3223})v_{rz}, \tag{2.17}$$

$$p_z^* = \mathcal{B}_{3232}v_{rr} + (r\mathcal{B}'_{3232} + \mathcal{B}_{3232})\frac{v_r}{r} + \mathcal{B}_{2222}v_{zz} + (\mathcal{B}_{2233} + \mathcal{B}_{3223})u_{rz}$$

$$+(r\mathcal{B}'_{3223} + r\bar{p}' + \mathcal{B}_{3223} + \mathcal{B}_{1122})\frac{u_z}{r}, \tag{2.18}$$

and the associated boundary conditions (2.16) become

$$v_r + u_z = 0, \quad \text{on } r = a, b, \tag{2.19}$$

$$(\mathcal{B}_{3333} - \mathcal{B}_{2233} + \lambda_3 W_3)u_r + (\mathcal{B}_{1133} - \mathcal{B}_{2233})\frac{u}{r} - p^* = 0, \quad \text{on } r = a, b. \tag{2.20}$$

In the above equations, a subscript on p^*, u or v denotes partial differentiation with respect to the implied coordinate (as indicated in (2.14)), and the primes denote d/dr.

For our illustrative calculations, we shall use three representative material models: the Ogden material model (Ogden, 1972), the Gent material model (Gent, 1996), and an arterial model, for which the strain-energy function is given, respectively, by

$$W = \mu \sum_{r=1}^{3} \mu_r^*(\lambda_1^{\alpha_r} + \lambda_2^{\alpha_r} + \lambda_3^{\alpha_r} - 3)/\alpha_r, \tag{2.21}$$

$$W = -\frac{\mu}{2}J_m \ln(1 - \frac{J_1}{J_m}), \quad J_1 = \lambda_1^2 + \lambda_2^2 + \lambda_3^2 - 3, \tag{2.22}$$

and

$$W = \frac{\mu}{2(1-k+k\alpha)}\left\{(1-k)J_1 + k\mathrm{e}^{\alpha J_1} - k\right\}, \tag{2.23}$$

where μ is the shear modulus for infinitesimal deformations,

$$\alpha_1 = 1.3, \quad \alpha_2 = 5.0, \quad \alpha_3 = -2.0, \quad \mu_1^* = 1.491, \quad \mu_2^* = 0.003, \quad \mu_3^* = -0.023,$$

and J_m, k, α are material constants. We shall take $J_m = 97.2$ which is typical for rubbers, and $k = 1/2, \alpha = 1/4$ which is a simple choice that gives us the desired behaviour that when the axial force is fixed the pressure does not have a maximum in uniform inflation. Without the first term $(1-k)J_1$ on the right hand side, equation (2.23) has been postulated by Delfino et al. (1997) as a possible model for arteries. This first term is added to represent the contribution from the matrix material. Although both the Gent and Ogden models are believed to be excellent models for rubber materials, it will be shown that they give different predictions for localized bulging in the large stretch regime.

3. Numerical determination of the bifurcation condition

As outlined in the Introduction, we now look for a solution of the form

$$u = f(r)\mathrm{e}^{\alpha z}, \quad v = g(r)\mathrm{e}^{\alpha z}, \quad p^* = h(r)\mathrm{e}^{\alpha z}. \tag{3.1}$$

On substituting this into the incremental equilibrium equations and boundary conditions, and then eliminating $g(r)$ and $h(r)$ in favor of $f(r)$, we find that $f(r)$ satisfies a single fourth-order ordinary differential equation and two boundary conditions, which are numbered in Haughton & Ogden (1979b) as (53), (54), and (55), respectively. For our purpose, it is more convenient to rewrite them in matrix form as

$$\frac{d\boldsymbol{y}}{dr} = A(r,\alpha)\boldsymbol{y}, \quad a \le r \le b, \tag{3.2}$$

$$B(r,\alpha)\boldsymbol{y} = 0, \quad \text{on } r = a, b, \tag{3.3}$$

where $\boldsymbol{y} = [f, f', f'', f''']^T$, and the coefficient matrices A and B are given by

$$A = \begin{bmatrix} 0 & 1 & 0 & 0 \\ 0 & 0 & 1 & 0 \\ 0 & 0 & 0 & 1 \\ a_{41} & a_{42} & a_{43} & a_{44} \end{bmatrix}, \quad B = \begin{bmatrix} -1-\alpha^2 r^2 & r & r^2 & 0 \\ b_{21} & b_{22} & b_{23} & r^3\zeta(r) \end{bmatrix}, \tag{3.4}$$

with $\zeta(r) = \mathcal{B}_{3232}$, and

$$\begin{aligned}
r^4\zeta(r)a_{41} &= 3\mathcal{B}_{3232} + \alpha^2 r^3(\mathcal{B}'_{1122} - \mathcal{B}'_{1133} - \mathcal{B}'_{2222} + \mathcal{B}'_{2233} + \mathcal{B}'_{3223}) \\
&\quad -3r\mathcal{B}'_{3232} + r^2\mathcal{B}''_{3232} + \alpha^2 r^2(\mathcal{B}_{1111} + \mathcal{B}_{2222} - 2\mathcal{B}_{1122} - 2\mathcal{B}_{3223}) \\
&\quad -\alpha^4 r^4\mathcal{B}_{2323} + \alpha^2 r^4(\mathcal{B}''_{3232} - \sigma''_{33}), \\
r^4\zeta(r)a_{42} &= \alpha^2 r^4(2\mathcal{B}'_{2233} + 2\mathcal{B}'_{3223} - \mathcal{B}'_{2222} - \mathcal{B}'_{3333}) + 3r^2\mathcal{B}'_{3232} - 3r\mathcal{B}_{3232} \\
&\quad +\alpha^2 r^3(2\mathcal{B}_{2233} + 2\mathcal{B}_{3223} - \mathcal{B}_{2222} - \mathcal{B}_{3333}) - r^3\mathcal{B}''_{3232}, \\
r^4\zeta(r)a_{43} &= r^4(2\alpha^2\mathcal{B}_{3223} + 2\alpha^2\mathcal{B}_{2233} - \alpha^2\mathcal{B}_{2222} - \mathcal{B}''_{3232} - \alpha^2\mathcal{B}_{3333}) \\
&\quad -3r^3\mathcal{B}'_{3232} + 3r^2\mathcal{B}_{3232}, \\
r^4\zeta(r)a_{44} &= -2r^4\mathcal{B}'_{3232} - 2r^3\mathcal{B}_{3232}, \\
b_{21} &= \alpha^2 r^2\left(\mathcal{B}_{2222} + \mathcal{B}_{1133} - \mathcal{B}_{1122} - \mathcal{B}_{2233} - r\mathcal{B}'_{3232} - \mathcal{B}_{3232} + \sigma_3 + r\sigma'_{33}\right) \\
&\quad -r\mathcal{B}'_{3232} + \mathcal{B}_{3232}, \\
b_{22} &= \alpha^2 r^3(\mathcal{B}_{2222} + \mathcal{B}_{3333} - \mathcal{B}_{3223} - 2\mathcal{B}_{2233} + \sigma_3) + r^2\mathcal{B}'_{3232} - r\mathcal{B}_{3232}, \\
b_{23} &= r^2\left(r\mathcal{B}'_{3232} + 2\mathcal{B}_{3232}\right).
\end{aligned}$$

We have solved this eigenvalue problem using both the determinant and compound matrix methods. It is found that the determinant method is sufficient for our current purpose because the problem is not stiff. All of our numerical computations and algebraic manipulations are carried out with the aid of *Mathematica* (Wolfram, 1991). Using the determinant

method, we first solve $B(a,\alpha)\boldsymbol{y}=0$ to find two linearly independent vectors, say $\boldsymbol{y}^{(1)}(a)$ and $\boldsymbol{y}^{(2)}(a)$. Next, we use each of these two vectors as an initial condition and integrate (3.2) from $r=a$ to $r=b$ to obtain two linearly independent solutions $\boldsymbol{y}^{(1)}(r)$ and $\boldsymbol{y}^{(2)}(r)$. Since a general solution can be written as a linear combination of these two solutions, satisfaction of the boundary condition at $r=b$ then requires that

$$E(\lambda_a,\alpha)\equiv \det\left\{B(b,\alpha)[\boldsymbol{y}^{(1)}(b),\boldsymbol{y}^{(2)}(b)]\right\}=0, \tag{3.5}$$

where the first equation defines the function $E(\lambda_a,\alpha)$, and $[\boldsymbol{y}^{(1)}(b),\boldsymbol{y}^{(2)}(b)]$ denotes the 4×2 matrix formed by putting the two vectors $\boldsymbol{y}^{(1)}(b)$ and $\boldsymbol{y}^{(2)}(b)$ side by side. Eigenvalues of α are the roots of $E(\lambda_a,\alpha)=0$. Thus, for each λ_a, we may iterate on α until the above error function is sufficiently small (typically smaller than 10^{-9}). In this way, the dependence of α on λ_a can be determined numerically. In the case of fixed axial force, the axial stretch λ_z is found to be a monotonically increasing function of λ_a, and can be taken as an independent parameter instead of λ_a.

As remarked in the Introduction, in general the eigen system (3.2) and (3.3) have both real and complex eigenvalues, but the distribution of eigenvalues of α in the complex α-plane must necessarily be symmetric with respect to both axes (since in the eigenvalue problem α appears through α^2 and all the coefficient functions are real). Such complex eigenvalues are computed in the context of determining the so-called edge-resonance modes in unstressed semi-infinite strips and cylinders; see, e.g., Zernov et al. (2006) and Pagneux (2011). For our current purpose, however, we only need to examine the real eigenvalues. It is found that there are five real eigenvalues as discussed in the Introduction. In Figure 2, we have shown a typical plot showing the variation of α_1^2 and α_2^2 with respect to λ_z when $A=0.9,\ F=0$, and when the Gent material model is used. It is seen that α_1^2 is positive when $\lambda_z<1.1889$ or $\lambda_z>3.3313$. We have verified, with the aid of (2.9), that these two intervals correspond to the two ascending branches of the pressure versus volume curve in uniform inflation, and it is precisely when $\lambda_z=1.1889$ or $\lambda_z=3.3313$ that the pressure attains its maximum or minimum, respectively. Thus, in the case of fixed axial force, localized bulging occurs when pressure reaches its maximum in uniform inflation. This correspondence has previously been proved analytically when the tube is modeled as a membrane without any bending stiffness (Fu & Il'ichev, 2015).

Figure 3 shows that the two outmost eigenvalues $\pm\alpha_2$ tend to infinity as the thickness tends to zero, which is consistent with the fact that when the membrane theory is used, there are only three real eigenvalues.

4. An explicit expression for the bifurcation condition

The numerical procedure used in the previous section breaks down when α is exactly equal to zero. In this section, we derive an analytical expression for the condition under which zero becomes a triple eigenvalue.

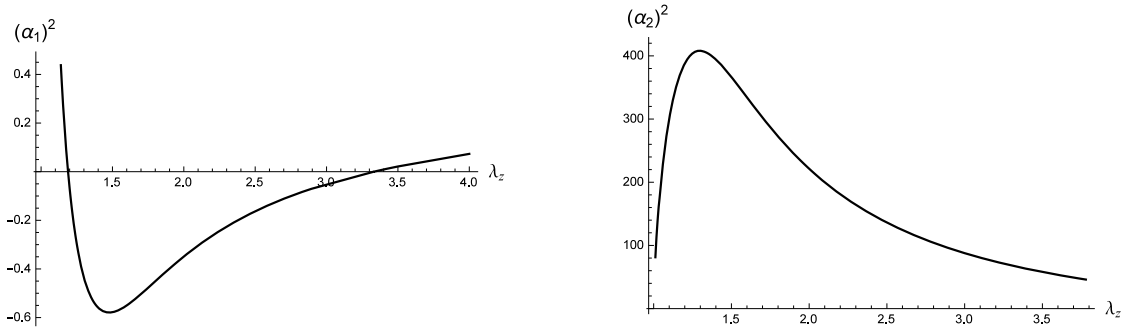

Figure 2: Variation of α_1^2 and α_2^2 with respect to λ_z when $A = 0.9,\ F = 0$, and when the Gent material model is used.

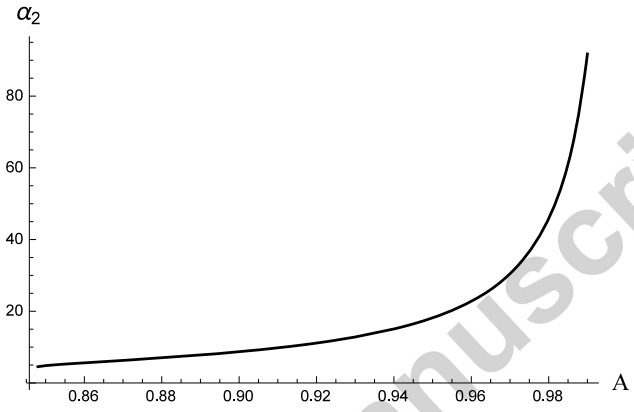

Figure 3: Variation of α_2 with respect to A, showing the fact that it tends to infinity in the thin-wall limit.

When α is small, we expand the coefficient matrix $A(r,\alpha)$ and $B(r,\alpha)$ in the form

$$A(r,\alpha) = A^{(0)}(r) + \alpha^2 A^{(1)}(r) + \cdots, \quad B(r,\alpha) = B^{(0)}(r) + \alpha^2 B^{(1)}(r) + \cdots, \tag{4.1}$$

and look for a solution of the form

$$\boldsymbol{y} = \boldsymbol{y}^{(0)} + \alpha^2 \boldsymbol{y}^{(1)} + \cdots, \quad f(r,\alpha) = f^{(0)}(r) + \alpha^2 f^{(1)}(r) + \cdots. \tag{4.2}$$

The explicit expressions for $A^{(0)}(r), B^{(0)}(r)$ etc are not written out here for the sake of brevity, and we recall that $f(r,\alpha)$ is the first element in $\boldsymbol{y}$. On substituting these expressions into (3.2) and (3.3), and equating the coefficients of α^0 and α^2 to zero, we obtain

$$\frac{d\boldsymbol{y}^{(0)}}{dr} = A^{(0)}(r)\boldsymbol{y}^{(0)}, \quad \frac{d\boldsymbol{y}^{(1)}}{dr} = A^{(0)}(r)\boldsymbol{y}^{(1)} + A^{(1)}(r)\boldsymbol{y}^{(0)}, \quad a \le r \le b, \tag{4.3}$$

$$B^{(0)}(r)\boldsymbol{y}^{(0)} = 0, \quad B^{(0)}(r)\boldsymbol{y}^{(1)} + B^{(1)}(r)\boldsymbol{y}^{(0)} = 0, \quad \text{on } r = a, b. \tag{4.4}$$

It can be deduced from $(4.3)_1$ that the fourth order differential equation satisfied by $f^{(0)}(r)$ can be rewritten in the compact form

$$\frac{d}{dr}\frac{1}{r}\frac{d}{dr}\left(r\zeta(r)\frac{d}{dr}\frac{1}{r}\frac{d}{dr}rf^{(0)}(r)\right) = 0, \tag{4.5}$$

so that a general solution can be deduced through straightforward integration and is given by

$$f^{(0)}(r) = c_1 r + c_2 \frac{1}{r} + c_3 \kappa_1(r) + c_4 \kappa_2(r), \tag{4.6}$$

where c_1, c_2, c_3, c_4 are constants and

$$\kappa_1(r) = \frac{1}{r}\int_a^r t \int_a^t \frac{s}{\zeta(s)} ds dt, \quad \kappa_2(r) = \frac{1}{r}\int_a^r t \int_a^t \frac{1}{s\zeta(s)} ds dt, \tag{4.7}$$

recalling that the function $\zeta(r)$ is defined below (3.4). On substituting this solution into the leading-order boundary condition $(4.4)_1$, it is found that the coefficients c_3 and c_4 must necessarily vanish, but c_1 and c_2 are unrestricted. At the next order, the general solution is given by

$$f^{(1)}(r) = d_1 r + d_2 \frac{1}{r} + d_3 \kappa_1(r) + d_4 \kappa_2(r) + c_1 \kappa_3(r) + c_2 \kappa_4(r), \tag{4.8}$$

where d_1, d_2, d_3, d_4 are constants and the last two terms are particular integrals given by

$$\kappa_3(r) = \frac{1}{r}\int_a^r y \int_a^y \frac{1}{x\zeta(x)} \int_a^x t \int_a^t \omega_1(s) ds dt dx dy, \tag{4.9}$$

$$\kappa_4(r) = \frac{1}{r}\int_a^r y \int_a^y \frac{1}{x\zeta(x)} \int_a^x t \int_a^t \omega_2(s) ds dt dx dy, \tag{4.10}$$

with $\omega_1(s)$ and $\omega_1(s)$ defined by

$$\begin{aligned}\omega_1(r) = {} & \mathcal{B}'_{1122} - \mathcal{B}'_{1133} + 3\mathcal{B}'_{2233} - 2\mathcal{B}'_{2222} - \mathcal{B}'_{3333} + 3\mathcal{B}'_{3223} + r(\mathcal{B}''_{3223} + \bar{p}'') \\ & + \frac{1}{r}(\mathcal{B}_{1111} - 2\mathcal{B}_{1122} + 2\mathcal{B}_{2233} - \mathcal{B}_{3333}), \\ \omega_2(r) = {} & \frac{1}{r}(\mathcal{B}''_{3223} + \bar{p}'') + \frac{1}{r^2}(\mathcal{B}'_{1122} - \mathcal{B}'_{1133} - \mathcal{B}'_{2233} - \mathcal{B}'_{3333} - \mathcal{B}'_{3223}) \\ & + \frac{1}{r^3}(\mathcal{B}_{1111} - 2\mathcal{B}_{1122} + 2\mathcal{B}_{2233} - \mathcal{B}_{3333}).\end{aligned}$$

On substituting (4.6) and (4.8) into the boundary condition $(4.4)_2$, we obtain a matrix equation of the form $M\boldsymbol{d} = 0$ where M is a 4×4 matrix which is not written out here for the sake of brevity, and $\boldsymbol{d}$ is the column vector formed from the four disposable constants c_1, c_2, d_3, d_4. It then follows that the condition for zero to become a triple eigenvalue is $\det M = 0$, which can be reduced to

$$\Omega(\lambda_a, \lambda_z) = 0, \tag{4.11}$$

where $\Omega(\lambda_a, \lambda_z)$ is given by

$$\begin{aligned}\Omega(\lambda_a, \lambda_z) = {} & 2\zeta(b)(F_1 - b^2 F_2 + D_1(b) - b^2 a^{-2} D_1(a) + D_2(a) - D_2(b)) \\ & -2\zeta(a)(F_1 - a^2 F_2 - D_1(a) + a^2 b^{-2} D_1(b) + D_2(a) - D_2(b)) \\ & +(1 - a^{-2}b^2) D_1(a)(F_1 - D_2(b)) + 2F_3(F_2 + a^{-2} D_1(a) - b^{-2} D_1(b)) \\ & +(1 - a^2 b^{-2}) D_2(a)(b^2 F_2 - D_1(b)) - 2F_4(F_1 + D_2(a) - D_2(b)),\end{aligned} \tag{4.12}$$

together with

$$F_1 = \int_a^b \omega_1(t)dt, \quad F_3 = \int_a^b t\left(\int_a^t \omega_1(s)ds\right)dt,$$

$$F_2 = \int_a^b \omega_2(t)dt, \quad F_4 = \int_a^b t\left(\int_a^t \omega_2(s)ds\right)dt.$$

$$D_1(r) = \mathcal{B}_{1122} - \mathcal{B}_{1133} - \mathcal{B}_{2233} + r\mathcal{B}'_{3223} + \mathcal{B}_{3333} + r\bar{p}' + \sigma_3,$$

$$D_2(r) = \mathcal{B}_{1122} - \mathcal{B}_{1133} - 2\mathcal{B}_{2222} + 3\mathcal{B}_{2233} + r\mathcal{B}'_{3223} + 2\mathcal{B}_{3223} - \mathcal{B}_{3333} + r\bar{p}' - \sigma_3.$$

The explicit bifurcation condition (4.11) is valid for all types of loading conditions imposed at the two ends. Guided by what is known in the case when the tube is modeled as a membrane and by the numerical calculations conducted in the previous section, we anticipate that there is some connection between (2.11) and (4.11). It turns out that the contour plots of $\Omega(\lambda_a, \lambda_z) = 0$ and $J(P, F) = 0$ in the (λ_a, λ_z)-plane always coincide. We therefore conclude that (2.11) and (4.11) are equivalent bifurcation conditions.

5. Effect of bending stiffness

With an explicit bifurcation condition at our disposal, we are now in a position to quantify precisely the effect of bending stiffness on the initiation pressure. We first summarize the main results when the tube is modeled as a membrane.

When a membrane tube is subjected to uniform inflation, the strain energy per unit surface area is given by $Hw(\lambda_1, \lambda_2)$, where H is the thickness in the undeformed configuration, w has the same meaning as in (2.2), and λ_1 and λ_2 are now the *constant* stretches in the azimuthal and axial directions, respectively. The bifurcation condition for the initiation of a localized bulge in an infinitely long tube without any imperfections is $\Omega^{(0)}(\lambda_1, \lambda_2) = 0$ with $\Omega^{(0)}(\lambda_1, \lambda_2)$ given by (6.2) in the next section; see also Fu et al. (2008, (6.2)). The pressure P_{mem} and axial force F_{mem} are given by

$$\frac{R_m}{H}P_{\text{mem}} = \frac{w_1}{\lambda_1\lambda_2}, \quad \frac{F_{\text{mem}}}{2\pi R_m H} = w_2 - \frac{\lambda_1 w_1}{2\lambda_2} \equiv \mu\hat{F}(\lambda_1, \lambda_2), \tag{5.1}$$

where R_m is the constant averaged radius in the undeformed configuration and the last equation defines the function $\hat{F}$. As discussed in Section 2, two commonly used loading conditions correspond to fixed axial stretch or fixed axial force, respectively. In the former case, the bifurcation condition $\Omega^{(0)}(\lambda_1, \lambda_2) = 0$ can be solved to find the value of λ_1, and hence the critical pressure, at which localized bulging takes place. In the latter case, $\hat{F} = \text{const}$ can be solved to express λ_2 as a function of λ_1. In the $\lambda_1\lambda_2$-plane, the curve corresponding to this function may be viewed as the *loading path* that starts from the point with coordinates $(1, 1)$. The contour plot of the bifurcation condition $\Omega^{(0)}(\lambda_1, \lambda_2) = 0$ gives another curve in the same plane. Localized bulging may take place only if these two curves have at least one intersection. In the case of fixed axial stretch, the loading path is simply a horizonal line in the $\lambda_1\lambda_2$-plane.

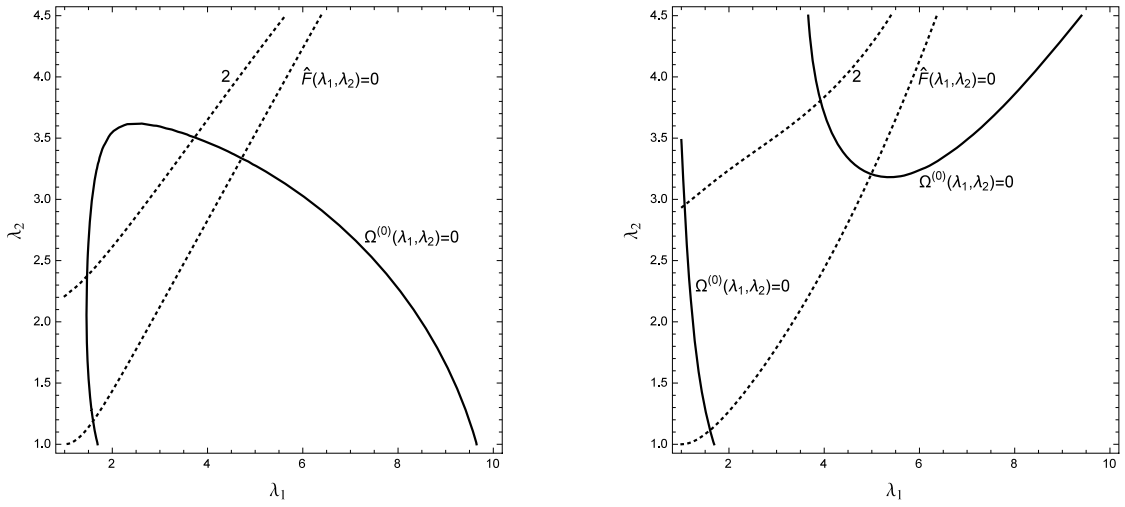

Figure 4: Results for a Gent material with $J_m = 97.2$ (left figure) and for the Ogden material (right figure). In both figures the loading curve $\hat{F}(\lambda_1, \lambda_2) = 0$ or 2 (shown in dotted line) and bifurcation condition $\Omega^{(0)}(\lambda_1, \lambda_2) = 0$ have two intersections, but they differ in that according to the Gent model localized bulging becomes impossible when the axial force or axial stretch becomes sufficiently large, whereas according to the Ogden model localized bulging is always possible.

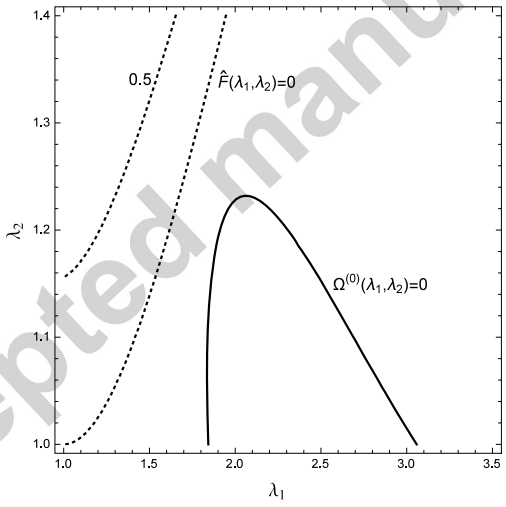

Figure 5: Results for the material model given by (2.23), showing the fact that $\hat{F}(\lambda_1, \lambda_2) = 0$ or 0.5 and $\Omega^{(0)}(\lambda_1, \lambda_2) = 0$ do not have any intersection and so localized bulging will not occur when $\hat{F}$ is fixed. However, localized bulging may still occur if it is the axial stretch that is held fixed during inflation.

Figures 4 and 5 depict two typical situations when such intersections may or may not take place, respectively. Fig.4(a, b) shows results typical of material models for which the pressure curve in uniform inflation has an N shape when the axial force is fixed. In this case, each of the two loading curves $\hat{F}(\lambda_1, \lambda_2) = 0, 2$ and the bifurcation condition $\Omega^{(0)}(\lambda_1, \lambda_2) = 0$ have two intersections, which correspond to the pressure maximum and

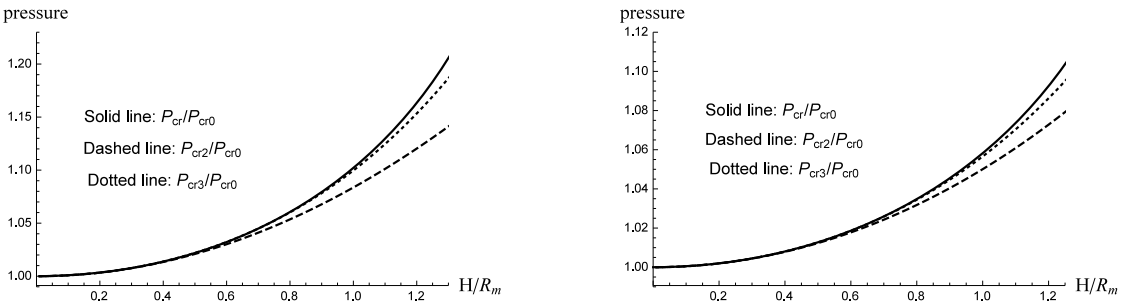

Figure 6: Comparison of the membrane theory with the exact theory and two other approximate theories that incorporate the effect of bending stiffness when the axial force is fixed at 0. The figures show variation of the initiation pressure for localized bulging as a function of the thickness/radius ratio when the Gent material model is used (left) or the Ogden material model is used (right).

minimum in uniform inflation, respectively. However, the Gent and Ogden material models give different predictions in the high stretch regime: whereas according to the Ogden model localized bulging is always possible, the Gent model predicts that localized bulging becomes impossible when the axial force or axial stretch becomes sufficiently large. This is due to the fact that for the Gent material model the two branches of $\Omega^{(0)}(\lambda_1, \lambda_2) = 0$ are joined at a finite value of λ_2 whereas for the Ogden material these two branches are never joined.

In contrast, Fig.5 shows results corresponding to the material model given by (2.23), which are typical of material models for which the pressure does not have a maximum when the axial force is fixed. In this case, there are no intersections, which means that the pressure would be monotonic in uniform inflation. However, these results demonstrate the fact that even if localized bulging cannot take place in the case of fixed axial force, it may still occur in the case of fixed axial stretch. In the latter case the loading path in the $\lambda_1\lambda_2$-plane is simply a horizontal line and it has intersections with $\Omega^{(0)}(\lambda_1, \lambda_2) = 0$ provided λ_2 does not exceed a threshold value (which is approximately equal to 1.23 in Fig.5).

We now proceed to discuss the effect of bending stiffness. We shall focus on the first bifurcation point, and use $P_{\rm cr}$ and $P_{\rm cr0}$ to denote the critical pressures predicted by the exact theory and membrane theory, respectively. Fig.6 shows how good the membrane theory is in predicting the critical pressure for localized bulging when $F = 0$: it shows how the critical pressure $P_{\rm cr}$, normalized by $P_{\rm cr0}$, varies with respect to H/R_m (the dashed and dotted lines, $P_{\rm cr2}$, and $P_{\rm cr3}$ in the figures will be defined in the next section). In the limit $H/R_m \to 0$, we have $P_{\rm cr}/P_{\rm mem} \to 1$ and so the membrane theory becomes exact. It can be seen that the membrane theory always under-predicts the initiation pressure, but due to the fact that the curve is very flat near $H/R_m = 0$ the error is less than 5% for values of H/R_m up to approximately 0.67.

Fig.7 shows how the contour plot of $\Omega(\lambda_a, \lambda_z) = 0$ evolves with respect to A (we have taken $B = 1$ without loss of generality). These results are based on the Gent material model

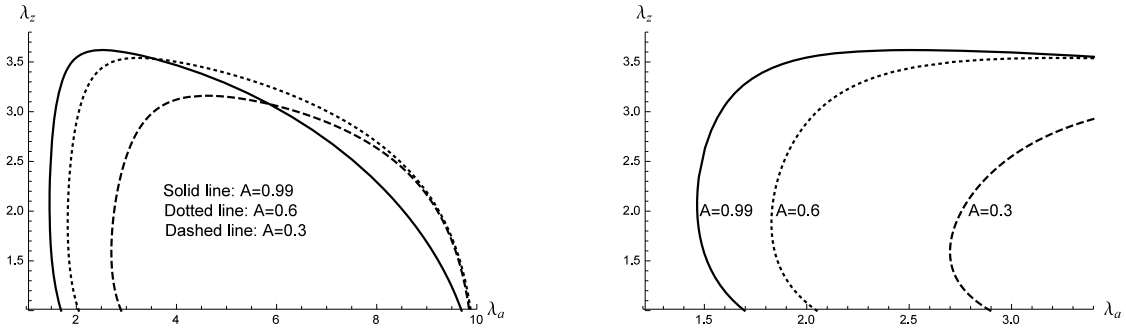

Figure 7: Evolution of the contour plot of $\Omega(\lambda_a, \lambda_z) = 0$ with respect to A when the Gent material model with $J_m = 97.2$ is used. The right plot shows a blow-up of the left plot near $\lambda_a = \lambda_z = 1$.

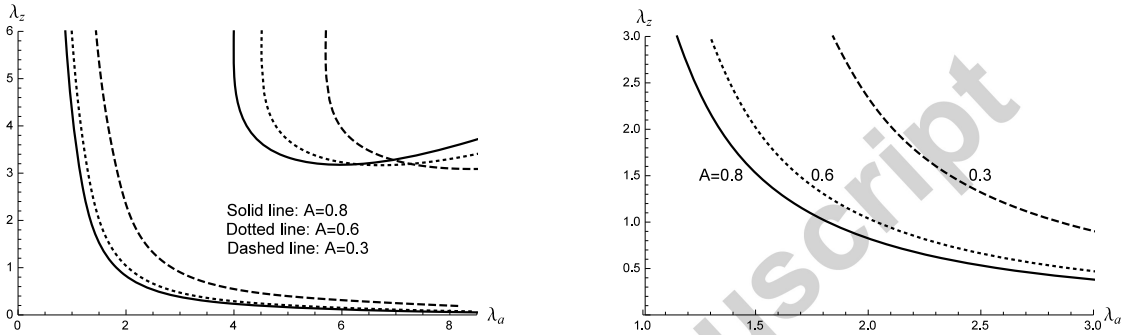

Figure 8: Evolution of the contour plot of $\Omega(\lambda_a, \lambda_z) = 0$ with respect to A when the Ogden material model is used. The right plot shows a blow-up of the left plot near $\lambda_a = \lambda_z = 1$.

with $J_m = 97.2$. The first curve corresponding to $A = 0.99$ is graphically indistinguishable from its membrane counterpart in Fig.4(a). It shows clearly that for each fixed λ_z, the larger the wall thickness, the greater the critical value of λ_a. Similar behavior can be observed in Fig.8 when the Ogden material model is used.

Fig.9 offers a different perspective on the results of Figs 7 and 8 by taking the horizontal axis as the normalized internal pressure defined by

$$\hat{P} = \frac{R}{\mu H} P, \tag{5.2}$$

where P is calculated using the expression (2.3). It shows that the normalized critical pressure is a decreasing function of the axial stretch. We also observe that at each fixed value of λ_z the normalized critical pressure would increase with respect to increase in the wall thickness, as expected, but such increases are almost negligible for values of A between 1 and 0.6. This is consistent with the observations made with regards Fig.6. Results shown in this figure can also be used directly to interpret the experimental results reported in Goncalves et al. (2008). The authors in the latter paper conducted a series of experiments on localized bulging in thick-walled cylindrical tubes with H/R_m ranging from 0.25 to 0.5, and with λ_z fixed at a number of values in turn. All of their results show that the initiation

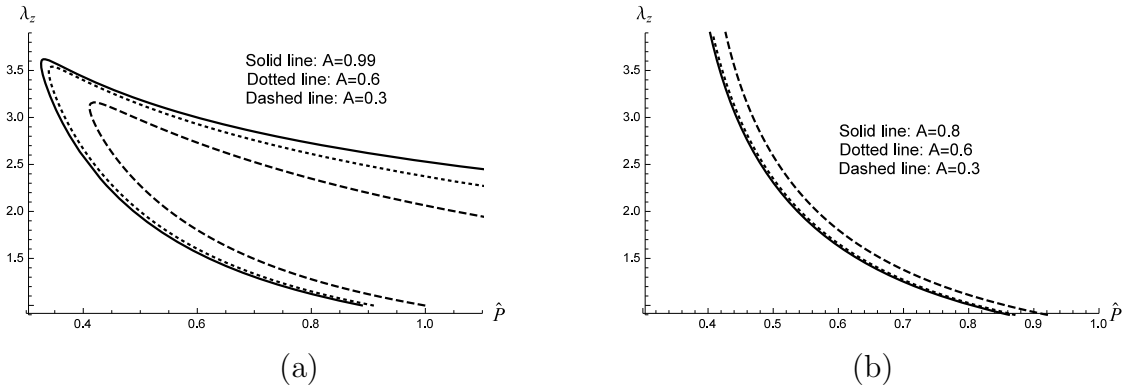

Figure 9: Variation of λ_z with respect to the normalized pressure $\hat{P}$ when $F = 0$. (a) When the Gent material model is used; (b) when the Ogden material model is used.

pressure decreases with increased λ_z, which is consistent with our theoretical predictions displayed in Fig.9. Similar behavior was also observed in the experimental study of Ma et al. (2014) on short-length tubular balloons. To make a quantitative comparison with the results of Goncalves et al. (2008), we consider the specimen that they numbered as B204. Using (5.2) together with their values for μ, A and B, and our Fig.9 to compute the dimensional initiation pressure (i.e. the values of P, rather than $\hat{P}$), we obtain 0.216, 0.189, and 0.168 (unit MPa) when λ_z is equal to $1, 1.16$ and 1.32, respectively. The corresponding values of the initiation pressure given by their Fig.7 are 0.194, 0.188, and 0.172. The agreement is very impressive, especially considering the fact that our choice of $J_m = 97.2$ do not necessarily fit their material. We observe, however, that in the above-mentioned paper the authors used a Mooney-Rivlin material model in their numerical simulations. It can be shown that according to this model, the critical pressure would increase when λ_z is increased, which would contradict their experimental results. Furthermore, the Mooney-Rivline material model is not suitable for modeling bulge initiation and propagation in another aspect: according this model the diameter at the center of the bulge would grow for ever once the bulge has initiated (because the pressure versus volume curve does not have a minimum so that a Maxwell state corresponding to steady propagation cannot be reached).

6. A two-term approximation incorporating the effect of bending stiffness

Although (4.11), or equivalently (2.11), can be used to compute the exact initiation pressure for localized bulging for any given material model, it involves integrals that in general do not have closed-form expressions. In this section, we shall derive a two-term approximation for this bifurcation condition that can be used to compute the initiation pressure with sufficient accuracy for values of H/R_m over a sufficiently large interval.

We first introduce the wall thickness $H = B - A$, averaged radius $R_m = (A + B)/2$, and

define a dimensionless parameter ε through

$$\varepsilon = \frac{H}{R_m}.$$

We then have

$$A = R_m - \frac{H}{2}, \quad B = R_m + \frac{H}{2}, \quad a = r_m - \frac{h}{2}, \quad b = r_m + \frac{h}{2},$$

where h and r_m are the tube wall thickness and the averaged radius in the deformed configuration, respectively. We also have

$$\lambda_a = (\lambda_m - \frac{\varepsilon}{2\lambda_m\lambda_z})(1-\frac{\varepsilon}{2})^{-1}, \quad \lambda_b = (\lambda_m + \frac{\varepsilon}{2\lambda_m\lambda_z})(1+\frac{\varepsilon}{2})^{-1},$$

where λ_m is the azimuthal stretch at $r = r_m$ and we have replaced H/h by $\lambda_m\lambda_z$. At first sight, one may think that $H/h = \lambda_m\lambda_z$ is only valid to leading order, but it turns out that the above expressions satisfy the incompressibility condition (2.4) exactly.

With the use of the above expressions, it is found that the $\Omega(\lambda_a, \lambda_z)$ in (4.11) may be expanded as

$$\Omega(\lambda_a, \lambda_z) = \varepsilon^2 \frac{4}{\lambda_m^3\lambda_z^2}\Omega^{(0)} + \varepsilon^4 \frac{1}{6\lambda_m^7\lambda_z^4}\Omega^{(1)} + O(\varepsilon^6), \tag{6.1}$$

where $\Omega^{(0)}$ and $\Omega^{(1)}$ are given by

$$\Omega^{(0)} = \lambda_m(w_1 - \lambda_z w_{12})^2 + \lambda_z^2 w_{22}(w_1 - \lambda_m w_{11}), \tag{6.2}$$

$$\begin{aligned}
\Omega^{(1)} \;=\; & 2\lambda_m(3+2\lambda_m^2\lambda_z)w_1^2 - 4\lambda_m^4\lambda_z(2-\lambda_m^2\lambda_z)w_1w_{11} - 8\lambda_m\lambda_z(1+\lambda_m^2\lambda_z)w_1w_{12} \\
& +6\lambda_z^2(1+\lambda_m^2\lambda_z)w_1w_{22} + 4\lambda_m^3\lambda_z^3w_{12}^2 + 2\lambda_m\lambda_z^2(1-\lambda_m^2\lambda_z)w_1w_{122} \\
& +2\lambda_m(1-\lambda_m^2\lambda_z)\left(\lambda_m^2(3-\lambda_m^2\lambda_z)w_1w_{111} - 2\lambda_m\lambda_z(1-\lambda_m^2\lambda_z)w_1w_{112}\right) \\
& \lambda_m^2\lambda_z(1-\lambda_m^2\lambda_z)^2\left(\lambda_z w_1w_{1122} - 2\lambda_m w_1w_{1112}\right) - 2\lambda_m^3(3-2\lambda_m^2\lambda_z)w_{11}^2 \\
& +\lambda_m\lambda_z(1+\lambda_m^2\lambda_z)\left(4\lambda_m(2-\lambda_m^2\lambda_z)w_{11}w_{12} - 6\lambda_z w_{11}w_{22}\right) \\
& +\lambda_m^2\lambda_z(1-\lambda_m^2\lambda_z)\left(4\lambda_m w_{11}w_{112} - 2\lambda_z w_{11}w_{122} + 3\lambda_z(1+\lambda_m^2\lambda_z)w_{111}w_{22}\right) \\
& +\lambda_m^3\lambda_z(\lambda_m^2\lambda_z - 1)\left(2(3-\lambda_m^2\lambda_z)w_{111}w_{12} + 4\lambda_m\lambda_z^2 w_{112}w_{12}\right) \\
& +\lambda_m^3\lambda_z^2(1-\lambda_m^2\lambda_z)^2(2w_{1112}w_{12} - w_{11}w_{1122} - w_{1111}w_{22}),
\end{aligned} \tag{6.3}$$

with all the partial derivatives of w evaluated at $\lambda_1 = \lambda_m$. As expected, the leading order result $\Omega^{(0)}(\lambda_m, \lambda_z) = 0$ is simply the bifurcation condition in the membrane approximation (Fu et al., 2008, (6.2)). With an error of order ε^4, the expression

$$\Omega^{(0)} + \frac{\varepsilon^2}{24\lambda_m^4\lambda_z^2}\Omega^{(1)} = 0 \tag{6.4}$$

then gives a two-term approximation to the bifurcation condition that incorporates the effect of bending stiffness.

To the same order of accuracy, we may expand the right hand sides of (2.3) and (2.6) to obtain

$$P = \varepsilon \frac{w_1}{\lambda_m \lambda_z} + \varepsilon^3 \frac{K_1}{24\lambda_m^3 \lambda_z^3} + O(\varepsilon^5), \tag{6.5}$$

$$\frac{F}{\pi(B^2 - A^2)} = w_2 - \frac{\lambda_m w_1}{2\lambda_z} + \varepsilon^2 \frac{K_2}{48\lambda_m^3 \lambda_z^3} + O(\varepsilon^4), \tag{6.6}$$

where the coefficients K_1 and K_2 are defined by

$$\begin{aligned} K_1 &= 2\lambda_z w_1 + 2(\lambda_m^3 \lambda_z^2 - \lambda_m \lambda_z) w_{11} + (1 + \lambda_m^4 \lambda_z^2 - 2\lambda_m^2 \lambda_z) w_{111}, \\ K_2 &= (\lambda_m^2 \lambda_z - 1) \left(2w_1 - 4w_{12}\lambda_z + 4w_{11}\lambda_m - 2w_{11}\lambda_m^3 \lambda_z + w_{111}\lambda_m^2 \right. \\ &\quad \left. + 2w_{112}\lambda_m^3 \lambda_z^2 - 2w_{112}\lambda_m \lambda_z - w_{111}\lambda_m^4 \lambda_z \right). \end{aligned}$$

As expected, the leading-order terms on the right hand sides of (6.5) and (6.6) correspond to the membrane approximation (5.1). The fact that the first correction term in (6.5) is of order ε^3 in some sense explains the excellent performance of the membrane theory as shown in Fig.6.

We note that an expansion similar to (6.5) was recently derived by Mangan & Destrade (2015). However, their expansion was in terms of H/A and their derivatives were evaluated at $\lambda_1 = \lambda_a$. As a result, their second term is quadratic in H/A.

On substituting (6.5) and (6.6) into the equivalent bifurcation condition (2.11) and keeping only the first two terms, we obtain

$$\Omega^{(0)} + \frac{\varepsilon^2}{24\lambda_m^3 \lambda_z^2} \Omega^{(2)} = 0, \tag{6.7}$$

where $\Omega^{(2)}$ is given by

$$\begin{aligned} \Omega^{(2)} &= 4w_1^2 \lambda_m^2 \lambda_z - (6 - 4\lambda_m^2 \lambda_z)(w_{11}^2 \lambda_m^2 + w_{12}^2 \lambda_z^2) + 3w_{111} w_{22} \lambda_m \lambda_z^2 (1 - \lambda_m^4 \lambda_z^2) \\ &\quad + \lambda_m \lambda_z (1 - \lambda_m^2 \lambda_z)^2 (2w_{1112} w_{12} \lambda_m \lambda_z - w_{1111} w_{22} \lambda_m \lambda_z - 4w_1 w_{112}) \\ &\quad + w_{12} \lambda_m^2 \lambda_z (\lambda_m^2 \lambda_z - 1)(2w_{111} \left(3 - \lambda_m^2 \lambda_z\right) + 4w_{112} \lambda_m \lambda_z^2) \\ &\quad + w_{11} \lambda_m \lambda_z^2 (-w_{1122} \lambda_m + 2w_{1122} \lambda_m^3 \lambda_z + 2w_{122} \lambda_m^2 \lambda_z - 6w_{22} \lambda_m \lambda_z - 2w_{122}) \\ &\quad + 4w_{11} w_{112} \lambda_m^2 \lambda_z (1 - \lambda_m^2 \lambda_z) - 4w_{11} w_{12} \lambda_m \lambda_z (\lambda_m^2 \lambda_z - 2)(\lambda_m^2 \lambda_z + 1) \\ &\quad + 2\lambda_z (1 - 2\lambda_m^2 \lambda_z)(2w_1 w_{12} - w_1 w_{1112} \lambda_m^2) + 2w_1 \lambda_m \lambda_z^3 (3w_{22} - w_{122} \lambda_m) \\ &\quad + w_1 \lambda_m^3 \lambda_z (\lambda_m^2 \lambda_z - 2)(4w_{11} + w_{1122} \lambda_z^2) + w_1 \lambda_m \lambda_z^2 (w_{1122} - 2w_{1112} \lambda_m^5 \lambda_z) \\ &\quad + 2w_1 \left\{ w_{111} \lambda_m^2 (1 - \lambda_m^2 \lambda_z)(3 - \lambda_m^2 \lambda_z) + w_{122} \lambda_z^2 \right\} - w_{11} w_{1122} \lambda_m^6 \lambda_z^4. \end{aligned}$$

We note that although the first terms in (6.4) and (6.7) are identical, the second terms may differ from each other by a quantity of order ε^4.

The two-term bifurcation condition (6.4) or (6.7), together with the associated two-term approximations (6.5) and (6.6) for the pressure and axial force, gives us a leading-order theory that incorporates the effect of bending stiffness. To demonstrate its accuracy, we

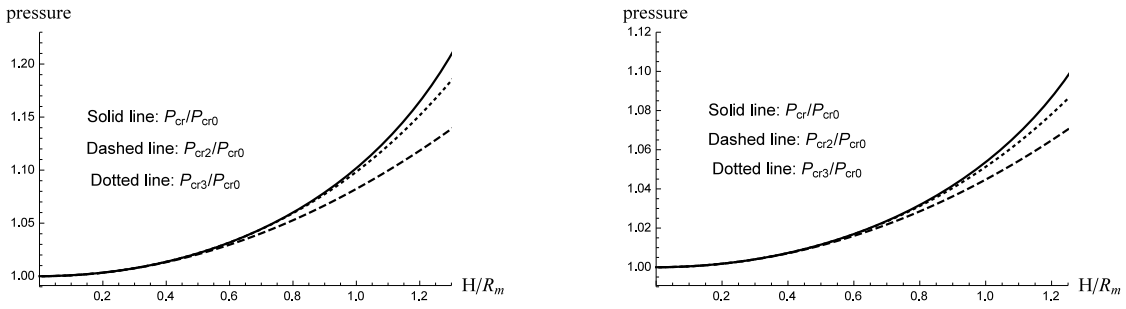

Figure 10: Comparison of the membrane theory with the exact theory and two other approximate theories that incorporate the effect of bending stiffness when the axial stretch λ_z is fixed at 1.1. (a) Results when the Gent material model is used; (b) results when the Ogden material model is used.

have shown its performance in Figs 6 and 10 for the cases of fixed axial force and fixed axial stretch, respectively, with $P_{\rm cr2}$ denoting the associated critical pressure. It is found in all cases that against the exact result the relative error in predicting the initiation pressure is less than 5% for values of H/R_m up to as large as 1.2. Similar results are obtained for the cases when the axial stretch is fixed to be 1.2, 1.4 and 1.6, respectively.

In Figs 6 and 10 we have also shown the results when the values of λ_m and λ_z are calculated using the two-term approximations (6.7) and (6.6) but the critical pressure, denoted by $P_{\rm cr3}$, is calculated using a three-term expansion with the third term given by

$$\frac{\varepsilon^5}{1920\lambda_m^5\lambda_z^5}\Big(24\lambda_z^2 w_1+24\lambda_m\lambda_z^2(\lambda_m^2\lambda_z+1)(\lambda_m^2\lambda_z-1)w_{11}+\left(\lambda_m^2\lambda_z-1\right)^4 w_{11111}$$

$$+12\lambda_z(3\lambda_m^2\lambda_z+1)(\lambda_m^2\lambda_z-1)^2 w_{111}+12\lambda_m\lambda_z(\lambda_m^2\lambda_z-1)^3 w_{1111}\Big)\,.$$

It is seen that there is significant improvement in the accuracy for the larger values of H/R_m. It is further found that with the values of λ_m and λ_z calculated using the two-term approximations but the critical pressure computed using the exact expression (2.3), the result in each case becomes graphically indistinguishable from the exact result for values of H/R_m up to as large as 1.33! To understand why the two-term bifurcation condition performs so well, we have shown in Fig.11 the contour plots of the exact bifurcation condition and its two-term approximation (6.7) for $\varepsilon = 0.22, 1.08$, respectively. It is seen that the two contour plots in each case are graphically indistinguishable in a sufficiently large part on the left; the two-term approximation only becomes increasingly poor in the large stretch regime as ε increases. Since it is the left part of the contour plot that is associated with the computation of the initiation pressure (see Fig.4 for two typical loading paths when the axial force is fixed and observe the fact when the axial stretch is fixed it is usually less than 2 in many applications), this explains why the two-term approximation (6.7) is almost exact as far as computation of the initiation pressure is concerned; the error mainly comes from the truncation of the power series expansion of the pressure.

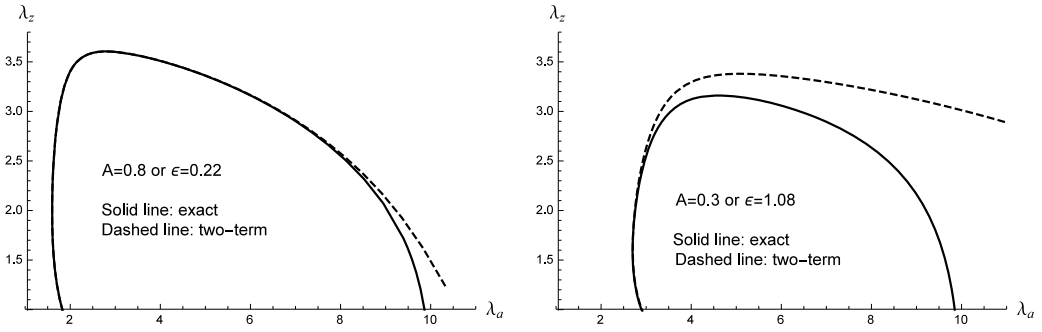

Figure 11: Comparison of the contour plots of the exact bifurcation condition and its two-term approximation (6.7) for $\varepsilon = 0.22, 1.08$.

7. Conclusion

This is our first study on localized bulging based on the exact theory of nonlinear elasticity. It is motivated by the fact that in some applications the cylindrical tube concerned may have walls thick enough so that the membrane theory may become invalid. Also, even if the membrane theory can be applied approximately it would be desirable to know precisely how good the approximation is. In this paper, an explicit bifurcation condition is derived for localized bulging in a cylindrical tube of arbitrary thickness. Using this explicit bifurcation condition, we are able to demonstrate that localized bulging is in fact possible for a cylindrical tube of arbitrary thickness. The initiation pressure varies linearly with respect to the wall thickness in the thin-wall limit, but this dependence becomes nonlinear for thick-walled tubes. It is also demonstrated that the membrane theory is surprisingly accurate as far as prediction of the initiation pressure is concerned: the error involved is less than 5% for wall thickness/radius ratios up to 0.67. A two-term approximation of the exact bifurcation condition is proposed, and is shown to be almost exact as far as the determination of the initiation pressure is concerned. The error mainly comes from the truncation of the power series expansion for the pressure: for thickness/radius ratios up to as large as 1.2, the relative error is less than 5% when two terms are kept in this expansion, and this error comes down to around 1% when three terms are kept in the expansion and to around 0.2% when the exact expression for the pressure is used. Thus, the two-term approximation of the exact bifurcation condition should be sufficient for all practical applications.

We conclude the paper by highlighting the fact that contrary to popular belief, *absence of the limit point instability does not imply non-existence of localized bulging*. The limit point instability exclusively refers to the case of fixed resultant axial force (which is usually zero, as when a party balloon is inflated), but one can envisage a number of other loading conditions under which the resultant axial force is not fixed. In particular, for arteries it is more appropriate to assume that it is the axial stretch that is fixed. Based on the results in Figs 4 and 5, it is not hard to see that localized bulging is likely to be possible for ALL

isotropic material models if the axial stretch is fixed to be below a certain threshold value that is dependent on the material model used. Whether localized bulging can take place or not can easily be verified by drawing the contour plot of the bifurcation condition as explained in the present paper.

Acknowledgements

This work was supported by the National Natural Science Foundation of China (Grant No 11372212).

References

Alexander, H. (1971). Tensile instability of initially spherical balloons. *Int. J. Eng. Sci.*, *9*, 151–160.

Alhayani, A. A., Giraldo, J. A., Rodríguez1, J., & Merodio, J. (2013). Computational modelling of bulging of inflated cylindrical shells applicable to aneurysm formation and propagation in arterial wall tissue. *Finite Elements in Analysis and Design*, *73*, 20–29.

Alhayani, A. A., Rodríguez, J., & Merodio, J. (2014). Competition between radial expansion and axial propagation in bulging of inflated cylinders with application to aneurysms propagation in arterial wall tissue. *Int. J. Eng. Sci.*, *85*, 74–89.

Chater, E., & Hutchinson, J. W. (1984). On the propagation of bulges and buckles. *ASME J. Appl. Mech.*, *51*, 269–277.

Chen, Y.-C. (1997). Stability and bifurcation of finite deformations of elastic cylindrical membranes - part i. stability analysis. *Int. J. Solids Struct.*, *34*, 1735–1749.

Delfino, A., Stergiopulos, N., Moore, J. E., & Meister, J.-J. (1997). Residual strain effects on the stress field in a thick wall finite element model of the human carotid bifurcation. *J. Biomech.*, *30*, 777–786.

Demirkoparan, H., & Merodio, J. (2015). Bulging bifurcation of inflated circular cylinders of doubly fiber-reinforced hyperelastic material under axial loading and swelling. *Math. Mech. Solids*, (p. DOI: 10.1177/1081286515600045).

Fu, Y. B., & Il'ichev, A. T. (2015). Localized standing waves in a hyperelastic membrane tube and their stabilization by a mean flow. *Maths Mech. Solids*, *20*, 1198–1214.

Fu, Y. B., Pearce, S. P., & Liu, K.-K. (2008). Post-bifurcation analysis of a thin-walled hyperelastic tube under inflation. *Int. J. Non-linear Mech.*, *43*, 697–706.

Fu, Y. B., Rogerson, G. A., & Zhang, Y. T. (2012). Initiation of aneurysms as a mechanical bifurcation phenomenon. *Int. J. Non-linear Mech.*, *47*, 179–184.

Fu, Y. B., & Xie, Y. X. (2010). Stability of localized bulging in inflated membrane tubes under volume control. *Int. J. Eng. Sci.*, *48*, 1242–1252.

Fu, Y. B., & Xie, Y. X. (2012). Effects of imperfections on localized bulging in inflated membrane tubes. *Phil. Trans. R. Soc., A 370*, 1896–1911.

Fung, Y. C., Froneck, K., & Patitucci, P. (1979). Pseudoelasticity of arteries and the choice of its mathematical expression. *Am. J. Physiol.*, *237*, H620–H631.

Gasser, T. C., Ogden, R. W., & Holzapfel, G. A. (2006). Hyperelastic modelling of arterial layers with distributed collage fibre orientations. *J.R. Soc. Interface*, *3*, 15–351.

Gent, A. (1996). A new constitutive relation for rubber. *Rubber Chem. Technol.*, *69*, 59–61.

Goncalves, P. B., Pamplona, D. C., & Lopes, S. R. X. (2008). Finite deformations of an initially stressed cylindrical shell under internal pressure. *Int. J. Mech. Sci.*, *50*, 92–103.

Haragus, M., & Iooss, G. (2011). *Local bifurcations, center manifolds, and normal forms in infinite-dimensional dynamical systems*. Springer, London.

Haughton, D. M., & Ogden, R. W. (1979a). Bifurcation of inflated circular cylinders of elastic material under axial loading i. membrane theory for thin-walled tubes. *J. Mech. Phy. Solids*, *27*, 179–212.

Haughton, D. M., & Ogden, R. W. (1979b). Bifurcation of inflated circular cylinders of elastic material under axial loading ii. exact theory for thick-walled tubes. *J. Mech. Phy. Solids*, *27*, 489–512.

Il'ichev, A. T., & Fu, Y. B. (2012). Stability of aneurysm solutions in a fluid-filled elastic membrane tube. *Acta Mechanica Sinica*, *28*, 1209–1218.

Kanner, L. M., & Horgan, C. O. (2007). Elastic instabilities for strain-stiffening rubber-like spherical and cylindrical thin shells under inflation. *Int. J. Non-linear Mech.*, *42*, 204–215.

Kirchgässner, K. (1982). Wave solutions of reversible systems and applications. *J. Diff. Eqns.*, *45*, 113–127.

Kyriakides, S., & Chang, Y.-C. (1990). On the inflation of a long elastic tube in the presence of axial load. *Int. J. Solids Struct.*, *26*, 975–991.

Kyriakides, S., & Chang, Y.-C. (1991). The initiation and propagation of a localized instability in an inflated elastic tube. *Int. J. Solids Struct.*, *27*, 1085–1111.

Lu, T. Q., An, L., Li, J. G., Yuan, C., & Wang, T. J. (2015). Electro-mechanical coupling bifurcation and bulging propagation in a cylindrical dielectric elastomer tube. *J. Mech. Phy. Solids*, *85*, 160–175.

Ma, G. Y., Li, T. F., Zou, Z. N., Qu, S. X., & Shi, M. X. (2014). Prestretch effect on snap-through instability of short-length tubular elastomeric balloons under inflation. *Int. J. Solids Strut.*, *51*, 2109–2115.

Mallock, A. (1891). Note on the instability of india-rubber tubes and balloons when distended by fluid pressure. *Proc. Roy. Soc.*, *A 49*, 458–463.

Mangan, R., & Destrade, M. (2015). Gent models for the inflation of spherical balloons. *Int. J. Non-linear Mech.*, *68*, 5258.

Mielke, A. (1991). *Hamiltonian and Lagrangian Flows on Center Manifolds, with Applications to Elliptic Variational Problems*. Springer-Verlag (Lecture Notes in Mathematics vol. 1489), Berlin.

Ogden, R. W. (1972). Large deformation isotropic elasticity on the correlation of theory and experiment for incompressible rubberlike solids. *Proc. Roy. Soc.*, *A 326*, 565584.

Pagneux, V. (2011). Complex resonance and localized vibrations at the edge of a semi-infinite elastic cylinder. *Math. Mech. Solids*, *17*, 17–26.

Pamplona, D. C., Goncalves, P. B., & Lopes, S. R. X. (2006). Finite deformations of cylindrical membrane under internal pressure. *Int. J. Mech. Sci.*, *48*, 683–696.

Pearce, S. P. (2012). Effect of strain-energy function and axial prestretch on the bulges, necks and kinks forming in elastic membrane tubes. *Math. Mech. Solids*, *17*, 860–875.

Pearce, S. P., & Fu, Y. B. (2010). Characterisation and stability of localised bulging/necking in inflated membrane tubes. *IMA J. Appl. Math.*, *75*, 581–602.

Rodrguez-Martnez, J. A., Fernndez-Sez, J., & Zaera, R. (2015). The role of constitutive relation in the stability of hyper-elasticspherical membranes subjected to dynamic inflation. *Int. J. Eng. Sci.*, *93*, 31–45.

Shi, J., & Moita, G. F. (1996). The post-critical analysis of axisymmetric hyper-elastic membranes by the finite element method. *Comput. Methods Appl. Mech. Engrg*, *135*, 265–281.

Shield, R. T. (1972). On the stability of finitely deformed elastic membranes; part ii: Stability of inflated cylindrical and spherical membranes. *ZAMP*, *23*, 16–34.

Wineman, A. S. (2015a). Determining the time of bulge formation in an elastomeric tube as it inflates, elongates and alters chemorheologically. *Math. Mech. Solids*, *20*, 924.

Wineman, A. S. (2015b). Bulge initiation in tubes of time-dependent materials. *Math. Mech. Solids*, (p. DOI: 10.1177/1081286515598827).

Wolfram, S. (1991). *Mathematica: A System for Doing Mathematics by Computer (2nd Edn)*. Addison-Wesley, California.

Yin, W.-L. (1977). Non-uniform inflation of a cylindrical elastic membrane and direct determination of the strain energy function. *J. Elast.*, *7*, 265–282.

Zernov, V., Pichugin, A. V., & Kaplunov, J. (2006). Eigenvalue of a semi-infinite elastic strip. *Proc. R. Soc., A 462*, 1255–1270.